Transient Stability of Single-Loop Voltage-Magnitude Controlled Grid-Forming Converters

Liu, Teng; Wang, Xiongfei

Published in:
IEEE Transactions on Power Electronics

DOI (link to publication from Publisher):
10.1109/TPEL.2020.3034288

Publication date:
2021

Document Version
Accepted author manuscript, peer reviewed version

Transient Stability of Single-Loop Voltage-Magnitude Controlled Grid-Forming Converters

Teng Liu, *Member, IEEE*, and Xiongfei Wang, *Senior Member, IEEE*

***Abstract*- This letter presents a design-oriented analysis on the transient stability of grid-forming (GFM) converters using single-loop voltage-magnitude (SLVM) control scheme. It is revealed that the used voltage-magnitude controller has a critical impact on the transient stability. This differs from the GFM converters using the vector-voltage control, whose transient stability is dominated by the outer power control loops. The theoretical findings are verified by experimental tests.**

***Index Terms*- Transient stability, grid-forming converters, single-loop voltage-magnitude control, phase portrait.**

I. Introduction

GRID-forming (GFM) converters are increasingly required by power system operators for the future power-electronic-based power systems [1]. The stability of GFM converters is of vital importance for the secure and resilient operation of power grids.

In contrast to the small-signal stability study [2], only a few studies on the transient stability of GFM converters, i.e., the ability of converters to maintain synchronism with the power system when subjected to large disturbances [3]-[5], have been reported. In [3], the transient stability of the GFM converter using the power synchronization control (PSC) is discussed, and it is proved that, due to its inherent first-order dynamic behavior, the system can maintain the synchronism as long as the equilibrium points exist. Yet, a constant voltage magnitude reference is assumed for the point of connection (PoC) voltage, and the impact of the *Q*-*V* droop control is overlooked in [3]. Recently, a general large-signal model for four typical GFM control schemes is reported in [4], which reveals that the *Q*-*V* droop controller can adversely affect the transient stability of GFM converter [5]. However, the dynamic impact of the inner voltage control loop is not considered in those transient stability studies, and it is assumed that the PoC voltage reference is ideally tracked within the timescale of transient stability. This assumption is justified when the fast-timescale vector-voltage control (VVC) is used [4]. Yet, it will not be valid when the single-loop voltage-magnitude (SLVM) control is used with the GFM converter [6]-[8], as will be shown in this letter.

The use of the SLVM control with GFM converter has been reported in the CERTS microgrid [6] and the high-voltage direct-current transmission systems interconnecting weak grids [7]. Differing from the VVC, the SLVM control regulates only the PoC voltage magnitude, while the phase angle generated by the *P*-*f* droop dictates the phase of the converter-bridge voltage before the output filter, rather than that of the PoC voltage. Consequently, the impact of the output filter, which is inherited in the VVC loop, has to be considered in the stability analysis of the SLVM control.

It is recently reported in [8] that the SLVM-controlled GFM converter has a better small-signal stability performance than that using the VVC, due to a larger coupling impedance introduced by the filter inductor. However, the impact of the SLVM control on the transient stability of GFM converter still remains as an open issue.

This letter attempts to fill the void. The impact of the SLVM control is analyzed, where the dynamic relationship between the converter-bridge voltage magnitude and the PoC voltage magnitude is derived. Then, by combining the dynamic of the voltage magnitude with that of the power control loops, the transient stability of the GFM converter is assessed by applying the phase portrait. The theoretical findings show that the SLVM control has a critical impact on the transient stability, which are further confirmed by the experimental tests.

II. Transient Stability Assessment of GFM Converter With SLVM Control

A. System Structure

Fig. 1(a) shows the single-line diagram of a grid-connected three-phase GFM converter with the SLVM control, where L_f and C_f constitute the converter output *LC* filter. L_g denotes the grid impedance. In GFM converters, the dc-side voltage control is usually taken over by either a front-end converter [7] or an energy storage unit [9] connected to the dc-link. A constant dc-link voltage is thus assumed in this study [3]-[5]. v is the converter-bridge voltage. v_{poc} and e are the PoC voltage and the grid voltage, respectively. i_g denotes the output current injected into the grid.

The droop control with the first-order low-pass filters (LPFs) is adopted as the outer power control in this letter. The output of the *Q*-*V* droop controller is used as the voltage magnitude reference V_{ref} for the SLVM control, which is given by

$$V_{ref} = K_q \left(Q_0 - Q \right) + V_0 \tag{1}$$

where K_q is the *Q*-*V* droop coefficient, V_0 is the rated voltage magnitude, Q and Q_0 are the filtered output reactive power of the GFM converter and its reference, respectively.

Then, the PoC voltage magnitude V_{poc} is regulated by the SLVM control to generate the converter-bridge voltage magnitude reference V, whose control law can be expressed as

$$V = k_{iv} \int \left(V_{ref} - V_{poc} \right) \tag{2}$$

where k_{iv} is the integral gain of the SLVM control.

Manuscript received August 23, 2020; revised October 06, 2020; accepted October 24, 2020. (*Corresponding author: Xiongfei Wang*)

The authors are with the Department of Energy Technology, Aalborg University, 9220 Aalborg, Denmark (e-mail: teli@et.aau.dk; xwa@et.aau.dk).

This article has been accepted for publication in a future issue of this journal, but has not been fully edited. Content may change prior to final publication. Citation information: DOI 10.1109/TPEL.2020.3034288, IEEE Transactions on Power Electronics

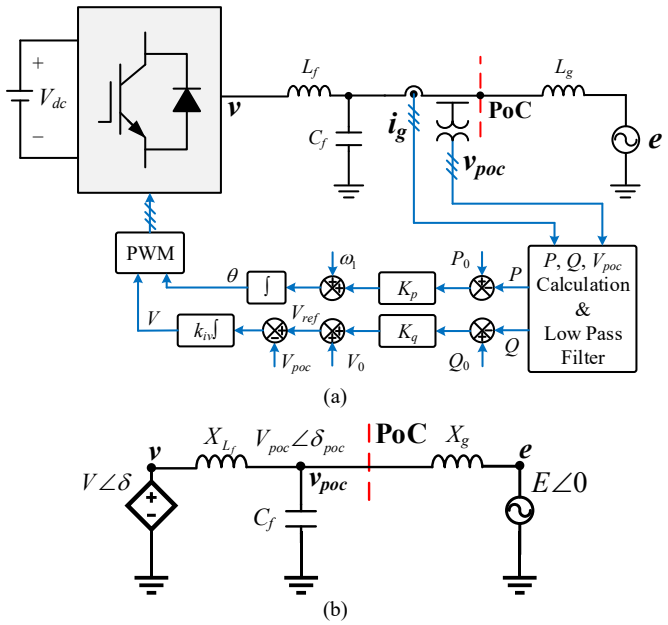

Fig. 1 (a) Single-line diagram of a grid-connected three-phase GFM converter with the SLVM control. (b) Simplified equivalent circuit.

Different from the VVC, the phase angle θ generated by the *P-f* droop controller determines the phase angle of v rather than that of v_{poc}, which is given by

$$\theta = K_p \int (P_0 - P) + \omega_1 t \tag{3}$$

where K_p is the *P-f* droop coefficient, ω_1 is the grid fundamental angular frequency, P and P_0 are the filtered output active power of the GFM converter and its reference, respectively.

Taking the phase angle of the grid voltage as the reference angle, the system equivalent circuit can be shown in Fig. 1(b). Since the SLVM control regulates the converter-bridge voltage v, rather than the filter capacitor voltage v_{poc} by using the VVC [8], the output *LC* filter should be considered in the transient stability analysis. δ denotes the power angle, which is the phase angle difference between v and e. Based on Fig. 1(b) and (3), its expression is derived as

$$\delta = \frac{K_p}{s} \cdot \frac{\omega_p}{s+\omega_p} \cdot \left(P_0 - \frac{3}{2} \cdot \frac{EV \sin\delta}{X_{L_f} + X_g} \right) \tag{4}$$

where the active power dissipated by the *LC* filter is neglected. ω_p is the cutoff frequency of the LPF.

B. Dynamic Representation of the GFM Converter

GFM converters are synchronized with the grid through the active power control loop, and thus the transient stability is determined by the dynamic response of the power angle δ under a large disturbance, which can be modeled by (4) with the condition that the converter output current will not exceed the overcurrent limit during the disturbances. Otherwise, the GFM control is switched to the vector current control to avoid the overcurrent [7], whose transient stability behavior is mainly determined by the used phase-locked loop (PLL), and has been well discussed in [10], [11]. Hence, only the transient stability

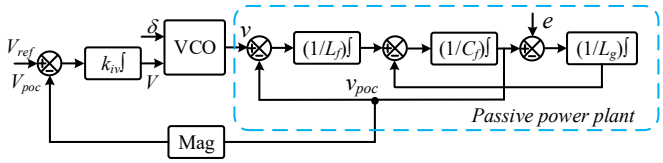

Fig. 2 Block diagram of the dynamic relationship between the converter-bridge voltage magnitude V and the PoC voltage magnitude V_{poc}.

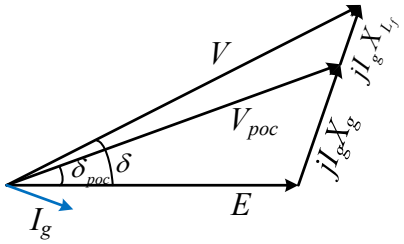

Fig. 3 Phasor diagram of the GFM converter without considering the effect of the filter capacitor.

of the GFM converter without triggering the overcurrent limit is focused in this work.

Applying the derivation on both sides of (4), the dynamic behavior of δ can be represented by

$$\ddot{\delta} = -\omega_p \dot{\delta} + \omega_p K_p \cdot \left(P_0 - \frac{3}{2} \cdot \frac{EV \sin\delta}{X_{L_f} + X_g} \right) \tag{5}$$

Different from the existing study in [3], V cannot be treated as a constant value. On the contrary, the dynamic of V, which is dependent on the SLVM control and the *LC* filter, is coupled with that of δ leading to a more complex dynamic behavior.

Recalling (1) and (2), the dynamic of V can be derived as

$$\dot{V} = k_{iv} \left[K_q \left(Q_0 - \frac{3}{2} \cdot \frac{V^2 - EV\cos\delta}{X_{L_f} + X_g} \right) + V_0 - V_{poc} \right] \tag{6}$$

C. Dynamic Relationship Between V and V_{poc}

Based on (5) and (6), to obtain the dynamic trajectory of δ under a large disturbance, the relationship between V and V_{poc} during transient states should be derived first. According to Fig. 1, there are two main factors responsible for their dynamic relationship. One is the SLVM control, another is the passive power plant consisting of the *LC* filter and grid impedance. The corresponding block diagram can be shown in Fig. 2.

In fact, the passive power plant shown in the dashed box follows the dynamic characteristic of the *LCL* filter network. Hence, if there is a step change in V, the dynamic response of V_{poc} will exhibit high-frequency damped oscillation considering the parasitic resistances of the passive components, and the oscillation frequency is equal to the *LCL* resonance frequency, which usually ranges from hundreds to thousands of Hertz.

On the other hand, the integrator of the SLVM control is known to have the LPF characteristic in the high frequency range. Due to its cascaded structure with the passive power plant shown in Fig. 2, the integral part of the SLVM control will "*filter out*" the high frequency dynamics caused by the filter capacitor. Therefore, the dynamic of the voltage magnitude is mainly dominated by the SLVM control.

This article has been accepted for publication in a future issue of this journal, but has not been fully edited. Content may change prior to final publication. Citation information: DOI 10.1109/TPEL.2020.3034288, IEEE Transactions on Power Electronics

Based on the above analysis, the phasor diagram of the GFM converter can be obtained by neglecting the filter capacitor, which is shown in Fig. 3. It should be noted that this phasor diagram is valid during transient states with the SLVM control. In this circumstance, V and V_{poc} will share the same dynamic behavior. Consequently, based on Fig. 3, the dynamic relationship between V and V_{poc} can be derived as

$$V_{poc}=\frac{\sqrt{E^2L_f^2+V^2L_g^2+2EVL_fL_g\cos\delta}}{L_f+L_g} \tag{7}$$

III. Phase Portrait-Based Transient Stability Analysis

A. Transient Stability Analysis with the SLVM Control

After obtaining the dynamic representation of the GFM converter with the SLVM control, the phase portrait [12], which shows the $\dot{\delta}-\delta$ curve, is applied for the transient stability assessment. The changing trend of δ after a large disturbance can be intuitively observed from the phase portrait, where δ will increase when $\dot{\delta}>0$ and decrease when $\dot{\delta}<0$. The points at which $\dot{\delta}=0$ are the equilibrium points (EPs). The transient stability will be achieved only when δ converges to a stable EP. Otherwise, the GFM converter will lose its synchronism with power grid.

By substituting (7) into (6), the dynamic of V can be rewritten as

$$\dot{V}=k_{iv}[K_q(Q_0-\frac{3}{2}\cdot\frac{V^2-EV\cos\delta}{X_{L_f}+X_g})+V_0 -\frac{\sqrt{E^2L_f^2+V^2L_g^2+2EVL_fL_g\cos\delta}}{L_f+L_g}] \tag{8}$$

Hence, due to the dynamic effect of the SLVM control, the synchronization stability of the GFM converter presents a three-dimensional dynamic behavior characterized by (5) and (8). By defining three state variables, i.e., $x_1=\delta$, $x_2=\dot{\delta}$, $x_3=V$, the differential equations given in (5) and (8) can be rewritten as

$$\begin{cases}\dot{x}_1=x_2\\ \dot{x}_2=-\omega_p x_2+\omega_p K_p\cdot\left(P_0-\frac{3}{2}\cdot\frac{E\cdot x_3\sin x_1}{X_{L_f}+X_g}\right)\\ \dot{x}_3=k_{iv}[K_q(Q_0-\frac{3}{2}\cdot\frac{x_3^2-E\cdot x_3\cos x_1}{X_{L_f}+X_g})\\ \quad +V_0-\frac{\sqrt{E^2L_f^2+x_3^2L_g^2+2E\cdot x_3L_fL_g\cos x_1}}{L_f+L_g}]\end{cases} \tag{9}$$

Then, the Matlab command "ode45" can be applied to solve (9), and the phase portraits are plotted in Fig. 4, where the main system parameters are summarized in Table I. It is known that the necessary condition for transient stability is that the system has EPs after the large disturbance [3]-[5]. In order to analyze the impact of the SLVM control on the transient stability, the first requirement is to guarantee existence of EPs. Since K_q will influence the EPs, its value is selected to guarantee existence of EPs. Further, the impact of K_p on the transient stability has been well studied in [4], where the decrease of K_p is expected to enhance the transient stability. Hence, the value of K_p, which can avoid possible transient instability caused by the P-f droop controller, is selected based on phase portrait.

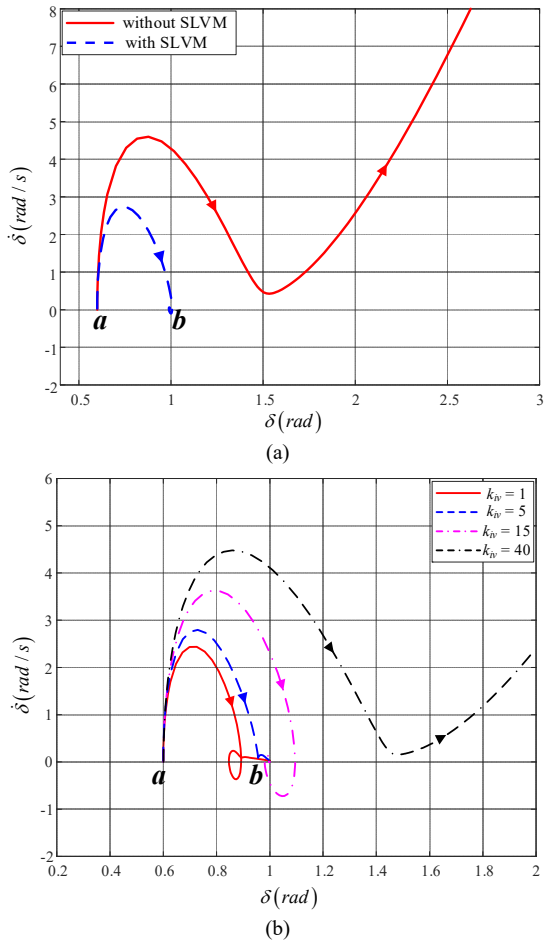

Fig. 4 Phase portraits of the GFM converter with the SLVM control (E drops from 1 p.u. to 0.6 p.u.) (a) comparison with the case without including the dynamic effect of the SLVM control. (b) Parametric effect of the integral gain k_{iv} on the transient stability.

TABLE I
Main System Parameters

Item	Symbol	Value
Grid voltage (l-g, rms)	e	50V (1.0 p.u.)
Grid fundamental frequency	f_1	50Hz
Switching frequency	f_{sw}	10kHz
Filter inductor	L_f	3mH (0.126 p.u.)
Filter capacitor	C_f	15μF (0.035 p.u.)
Grid impedance	L_g	10mH (0.419 p.u.)
Rated active power	P_0	1kW (1.0 p.u.)
Rated reactive power	Q_0	0Var
P-f droop coefficient	K_p	$0.05\omega_1/P_0$ (0.05 p.u.)
Q-V droop coefficient	K_q	$0.10V_0/P_0$ (0.10 p.u.)

Fig. 4(a) shows the phase portraits with and without the dynamic effect of the SLVM control, where the grid voltage magnitude E drops from 1 p.u. to 0.6 p.u. to emulate a grid fault. Point a denotes the stable EP of the system before the fault. It is observed that the transient stability assessment including the dynamic of the SLVM control predicts a stable result with δ

This article has been accepted for publication in a future issue of this journal, but has not been fully edited. Content may change prior to final publication. Citation information: DOI 10.1109/TPEL.2020.3034288, IEEE Transactions on Power Electronics

converging to a new stable EP *b* after the fault. On the contrary, when the dynamic effect of the SLVM control is neglected, i.e., a constant V is assumed, an opposite prediction is observed with the divergence of δ. Hence, the SLVM control has a critical impact on the transient stability of the GFM converter. Besides, it can also be concluded that, compared with the open-loop voltage control adopted in the synchronverter [9], the SLVM control can enhance the transient stability.

B. Parametric Influence of the SLVM Control

Further, the effect of the integral gain k_{iv} of the SLVM control on the transient stability is illustrated in Fig. 4(b). With the increase of k_{iv}, δ will exhibit larger overshoot, or even lose the synchronism when k_{iv} = 40. Therefore, a smaller integral gain means larger damping benefiting the transient stability, while the settling time for δ to reach the steady state will be slightly increased. Besides, the phase portraits of three stable cases all converge to the stable EP *b*, which means the position of the EPs will not be influenced by the SLVM controller parameters.

It is also worth mentioning that, even though this letter adopts the droop control with the LPFs as the outer power control loop, the analysis method can be readily applied to the other GFM control schemes.

IV. Experimental Results

To verify the theoretical findings, the experimental tests are conducted, where the system parameters listed in Table I are applied for the setup. The experimental setup is shown in Fig. 5. The power grid is emulated by a *Chroma Grid Simulator* 61845.

Fig. 6 shows the experimental dynamic responses of the GFM converter, where the three-phase grid voltage drops to 0.6 p.u. From Fig. 5(6), the GFM converter with the SLVM control can keep synchronism with the grid and reach to a new steady state after grid voltage sag. This stable phenomenon confirms the transient stability prediction given by the phase portrait in the dashed blue line in Fig. 4(a). Besides, when the SLVM control is intentionally disabled, the GFM converter will lose synchronism with the grid as shown in Fig. 6(b). Hence, it is verified that, compared with the open-loop voltage control [9], the SLVM control will enhance the transient stability.

Fig. 7 shows the experimental dynamic response of the GFM converter with the SLVM control when different integral gain

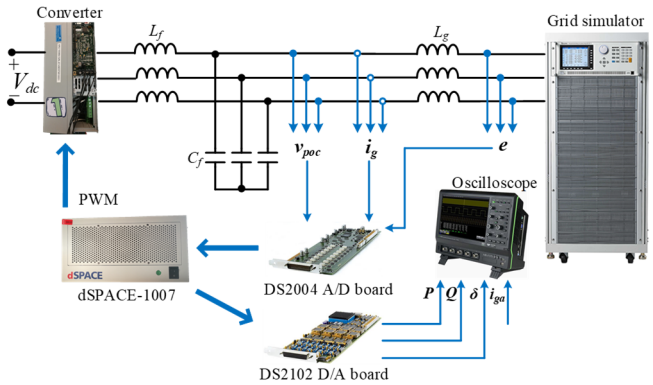

Fig. 5 Configuration of the experimental setup.

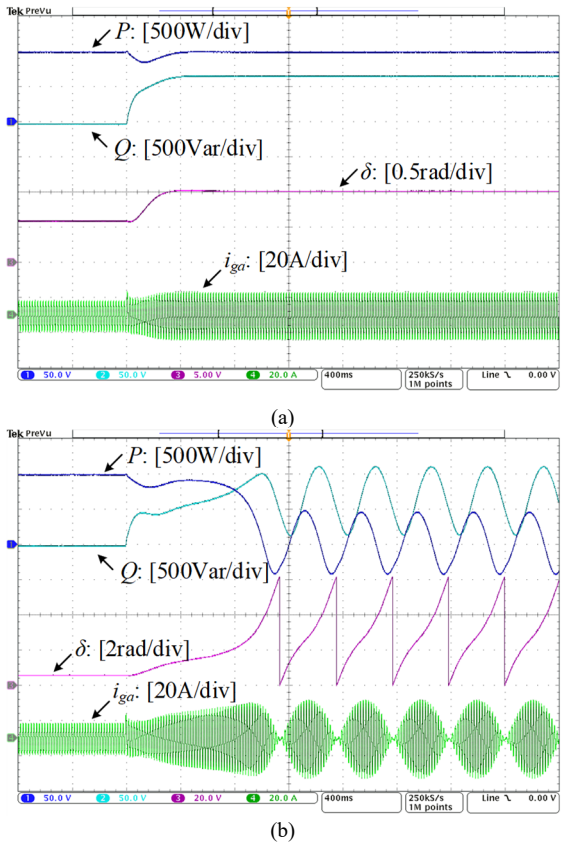

Fig. 6 Experimental dynamic responses of the GFM converter with the SLVM control (E drops from 1 p.u. to 0.6 p.u.) (a) the SLVM control is enabled. (b) the SLVM control is intentionally disabled.

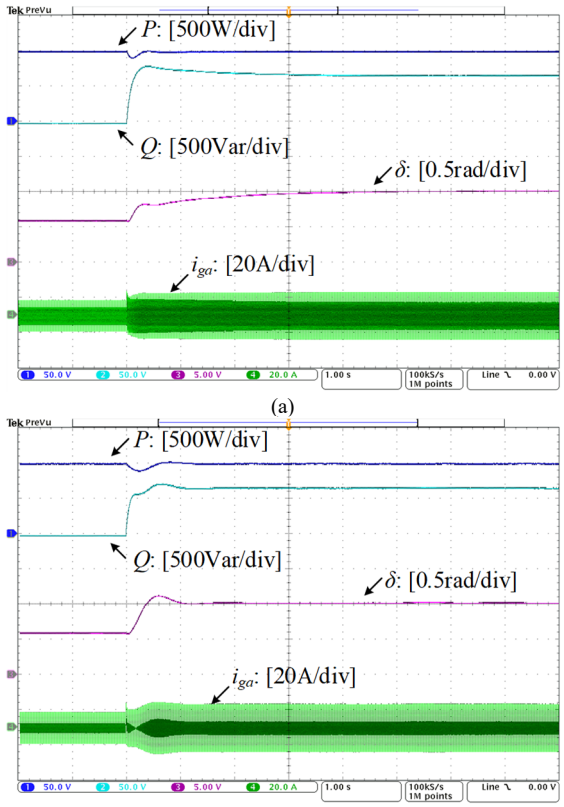

This article has been accepted for publication in a future issue of this journal, but has not been fully edited. Content may change prior to final publication. Citation information: DOI 10.1109/TPEL.2020.3034288, IEEE Transactions on Power Electronics

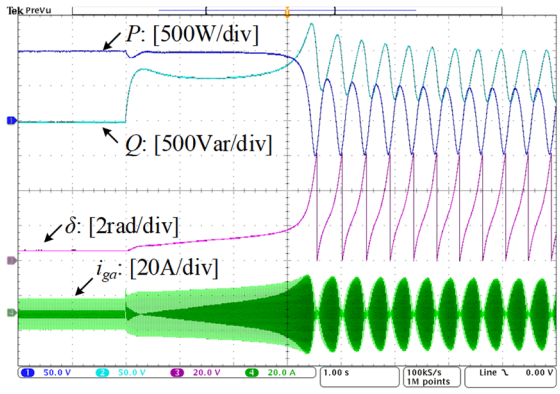

(c)

Fig. 7 Experimental dynamic responses of the GFM converter with the SLVM control (E drops from 1 p.u. to 0.6 p.u.) (a) $k_{iv} = 1$. (b) $k_{iv} = 15$. (c) $k_{iv} = 40$.

k_{iv} of the SLVM control is applied. It can be seen that, with the increase of k_{iv}, the dynamic response of δ shows larger overshoot, or even lose the synchronism with the grid when $k_{iv} = 40$. On the contrary, a smaller k_{iv} can provide larger damping with longer settling time. These experimental results coincide with the phase portraits depicted in Fig. 4(b), which further confirms the correctness of the theoretical findings.

V. Conclusions

This letter discusses the transient stability of GFM converters with the SLVM control. The phase-portrait analyses illustrate that the voltage-magnitude controller cannot be decoupled from the power-angle control, and it thus has a critical impact on the transient stability. Further, to enhance the transient stability, a small integral gain in the SLVM controller is recommended. The experimental tests verify the theoretical findings.

References

[1] R. H. Lasseter, Z. Chen, and D. Pattabiraman, "Grid-Forming Inverters: A Critical Asset for the Power Grid," *IEEE J. Emerg. Select. Topics Power Electron.*, vol. 8, no. 2, pp. 925-935, Jun. 2020.

[2] X. Wang and F. Blaabjerg, "Harmonic Stability in Power Electronic-Based Power Systems: Concept, Modeling, and Analysis," *IEEE Trans. Smart Grid*, vol. 10, no. 3, pp. 2858–2870, May 2019.

[3] H. Wu and X. Wang, "Design-Oriented Transient Stability Analysis of Grid-Connected Converters with Power Synchronization Control," *IEEE Trans. Ind. Electron.*, vol. 66, no. 8, pp. 6473-6482, Aug. 2019.

[4] D. Pan, X. Wang, F. Liu, and R. Shi, "Transient Stability of Voltage-Source Converters with Grid-Forming Control: A Design-Oriented Study," *IEEE J. Emerg. Select. Topics Power Electron.*, vol. 8, no. 2, pp. 1019-1033, Jun. 2020.

[5] D. Pan, X. Wang, F. Liu, and R. Shi, "Transient Stability Impact of Reactive Power Control on Grid-Connected Converters," in *Proc. IEEE ECCE*, Baltimore, 2019, pp. 4311-4316.

[6] E. Alegria, T. Brown, E. Minear, and R. H. Lasseter, "CERTS Microgrid Demonstration with Large-Scale Energy Storage and Renewable Generation," *IEEE Trans. Smart Grid*, vol. 5, no. 2, pp. 937-943, Mar. 2014.

[7] L. Zhang, L. Harnefors, and H. Nee, "Power-Synchronization Control of Grid-Connected Voltage-Source Converters," *IEEE Trans. Power Syst.*, vol. 25, no. 2, pp. 809-820, May 2010.

[8] W. Du, Z. Chen, K. P. Schnerider, R. H. Lasseter *et al.*, "A Comparative Study of Two Widely Used Grid-Forming Droop Controls on Microgrid Small-Signal Stability," *IEEE J. Emerg. Select. Topics Power Electron.*, vol. 8, no. 2, pp. 963-975, Jun. 2020.

[9] Q. Zhong, P. Nguyen, Z. Ma, and W. Sheng, "Self-Synchronized Synchronverters: Inverters Without a Dedicated Synchronization Unit," *IEEE Trans. Power Electron.*, vol. 29, no. 2, pp. 617-630, Feb. 2014.

[10] H. Wu and X. Wang, "Design-Oriented Transient Stability Analysis of PLL-Synchronized Voltage-Source Converters," *IEEE Trans. Power Electron.*, vol. 35, no. 4, pp. 3573-3589, Apr. 2020.

[11] H. Xin, L. Huang, L. Zhang, Z. Wang, and J. Hu, "Synchronous Instability Mechanism of *P-f* Droop-Controlled Voltage Source Converter Caused by Current Saturation," *IEEE Trans. Power Syst.*, vol. 31, no. 6, pp. 5206-5207, Nov. 2016.

[12] S. H. Strogatz. *Nonlinear Dynamics and Chaos: With Applications to Physics, Biology, Chemistry, and Engineering*. New York, NY, USA: Perseus Books, 1994.